Polymer 53 (2012) 3462–3468

Contents lists available at SciVerse ScienceDirect

Polymer

journal homepage: www.elsevier.com/locate/polymer

Molecular brushes with extreme grafted side chain densities

Jae Min Bak [a], Gourishanker Jha [a], Eungjin Ahn [b], Seo-Hyun Jung [c], Han Mo Jeong [a], Byeong-Su Kim [b], Hyung-il Lee [a,*]

[a] Department of Chemistry, University of Ulsan, Ulsan 680-749, Republic of Korea
[b] Interdisciplinary School of Green Energy and School of NanoBioscience and Chemical Engineering, UNIST (Ulsan National Institute of Science and Technology), Ulsan 689-798, Republic of Korea
[c] Research Center for Green Fine Chemicals, Korea Research Institute of Chemical Technology, Ulsan 681-802, Republic of Korea

ARTICLE INFO

Article history:
Received 30 March 2012
Received in revised form
30 May 2012
Accepted 4 June 2012
Available online 15 June 2012

Keywords:
ATRP
Molecular brushes
Initiation efficiency

ABSTRACT

A series of densely grafted poly(*n*-butyl acrylate) (PBA) molecular brushes with four different grafting densities were synthesized by the "grafting-from" approach using atom transfer radical polymerization (ATRP). A novel monomer, isopropylidene-2,2-Bis(methoxy)propionic hydroxyethylmethacrylate (IMPHMA), was synthesized and copolymerized with methyl methacrylate (MMA) under different monomer feed ratios to yield a series of linear poly(methyl methacrylate-*stat*-IMAPA), [PMMA-*s*-(PIMPHMA)]. The resulting copolymers were deprotected and transformed to macroinitiators, [PMMA-*s*-(PHEMA-IMPHMA-Br)]. n-Butyl acrylate (BA) was grafted from these macroinitiators to yield a series of molecular brushes, [PMMA-*s*-{(PIMPHMA)-*g*-PBA}], with various side chain lengths. Molecular brushes were characterized by gel permeation chromatography (GPC) and ^{1}H NMR. PBA side chains were cleaved by acid hydrolysis, and the resulting linear PBA polymers were characterized by GPC to study initiation efficiency during the synthesis of molecular brushes. The initiation efficiency increased with polymerization time and decreased with macroinitiators that had more initiation sites. Atomic force microscopy (AFM) measurements demonstrated the characteristic molecular structure by resolving individual brush molecules.

1. Introduction

It is well known that the shape of polymer molecules is an important factor that determines their properties [1]. During the last decade, polymer scientists have introduced a new philosophy of "molecular brushes" and synthesized more densely grafted molecular brushes [2–5]. The unique physical and chemical properties of molecular brushes offer potential applications in various fields including supersoft elastomers [6], precursors to nanowires or nanotubes [7–9], photonic crystals [10,11], and molecular tensile machines [12].

The properties of polymer brushes can be controlled by variation in grafting density and length of backbone and side chains [13–15]. It has been recently reported that the carbon–carbon covalent bonds of the backbone of molecular brushes can spontaneously break upon adsorption onto a substrate due to the tension generated by attractive interaction between the side chains and the substrate [12,16,17]. This tension governs the extent and rate of backbone scission. Tension depends on grafting density, length of side chains, and extent of substrate attraction [18]. This behavior has been observed for brushes with a fairly long backbone (DP of backbone = 2000–3000) and side chains (DP of side chains = 130–150). While the influences of side chain lengths and substrate attraction on scission have been extensively studied, fewer studies have focused on the effect of grafting density.

Molecular brushes have been synthesized by three methods: grafting-onto [19], grafting-through [20–22], and grafting-from [23–25]. The grafting-from method has been extensively studied due to its ability to prepare brushes with high grafting density from a backbone with a predetermined number of initiation sites. Generally, a backbone macroinitiator for the grafting-from approach contains one initiation site per monomer repeating unit. However, it is necessary to design a macroinitiator that has more than one initiation site per repeating unit to investigate how fast molecular brushes degrade with increasing grafting density. In this paper, we report the synthesis of molecular brushes with extreme grafted side chain density. In addition, we report on the trend of initiation efficiency [26] with respect to the number of

* Corresponding author.
E-mail address: sims0904@ulsan.ac.kr (H.-i. Lee).

0032-3861/$ – see front matter © 2012 Elsevier Ltd. All rights reserved.
http://dx.doi.org/10.1016/j.polymer.2012.06.008

initiation sites related to a steric interaction. For this purpose, we synthesized a protected monomer that can potentially offer two initiation sites. Polymerization of this monomer followed by deprotection and esterification led to a macroinitiator with two ATRP [27–32] initiation sites per repeating unit. The initiation efficiency during brush polymerization from various macroinitiators with different initiation site densities is discussed.

2. Experimental

2.1. Materials

All chemicals were purchased from Aldrich Chemical Co. or Tokyo Chemical Industry Co. Ltd. (TCI) and used as received unless otherwise stated. 2-Hydroxyethyl methacrylate (HEMA), N-N-N′-N′-N′-pentamethyldiethylenetriamine (PMDETA), 1-Ethyl-3-(3-dimethylaminopropyl)-carbodiimide (EDC), N-N′-dicyclohexylcarbondimide (DCC), and anisole were purchased from TCI. 2,2-Bis(hydroxymethyl) propanoic acid (2-Bis-MPA) (98%), p-Toluene sulphonic acid (TsOH) (98.5%), 2-,2-dimethoxypropane (98%), 4-Dimethylaminopyridine (DMAP) (99%), ethyl 2-bromoisobutyrate (98%) (EBiB), 0.1 N Hydrochloric acid, 2-bromo-2-methyl propionic acid (98%), Methyl methacrylate (MMA), *n*-butyl acrylate (BA), 1-butanol (99.8%), and conc. sulfuric acid were purchased from Aldrich. Copper (I) Bromide (CuBr) was purified by washing with glacial acetic acid, followed by washing with ethanol and acetone, and then dried under vacuum.

2.2. Instrumental

The apparent molecular weight and molecular weight distributions of polymers were measured on a GPC (Agilent technologies 1200 series) using polystyrene standard with DMF as the eluent at 30 °C and a flow rate of 1.00 mL/min ^{1}H NMR spectra were collected in DMF-d_7 and $CDCl_3$ on a Bruker avance 300 MHz NMR spectrometer. The morphology of the samples was investigated using atomic force microscopy (AFM, Nanoscope V, Veeco) via a tapping mode.

2.3. Synthesis

2.3.1. Isopropylidene-2,2-Bis(methoxy)propionic acid (I-Bis-MPA) [33]

10.00 g (74.55 mmol) of 2,-2 Bis (hydroxyl methyl) propanoic acid (Bis-MPA), 13.8 mL (111.83 mmol) of 2,2-dimethoxypropane, and 0.71 g (3.73 mmol) of *p*-toluenesulfonic acid monohydrate were dissolved in 50 mL of acetone. The reaction mixture was stirred for 2 h at room temperature. Approximately 5 mL of an NH_3/EtOH (2 M) solution was then added to neutralize the catalyst, and the solvent was evaporated at room temperature. The residue was then dissolved in (250 mL) CH_2Cl_2 and extracted with two portions of (20 mL) water. The organic phase was dried with $MgSO_4$ and evaporated to give I-Bis-MPA as white crystals: 11.7 g (90%). ^{1}H NMR (300 MHz, $CDCl_3$, δ in ppm): 1.18 (s, 3H, $-CH_3$), 1.40 (s, 3H, $-CH_3$), 1.43 (s, 3H, $-CH_3$), 3.64 (d, 2H, $-CH_2O$), 4.14 (d, 2H, $-CH_2O$).

2.3.2. Isopropylidene-2,2-Bis(methoxy)propionic hydroxyethylmethacrylate (IMPHMA)

3.40 g (19.50 mmol) of I-Bis-MPA, 2.21 g (17 mmol) of 2-hydroxyethyl methacrylate, and 0.244 g (2 mmol) of DMAP were mixed in 50 mL of CH_2Cl_2. The reaction flask was kept in an ice bath for 30 min and 3.74 g (19.50 mmol) EDC was then added. Stirring at room temperature was continued for 45 h. Once the reaction was complete, the product was washed with water three times to remove water-soluble urea salt. The crude product was purified by liquid chromatography on silica gel, eluting with hexane and ethyl acetate to 1:2 to give IMPHMA as a colorless viscous liquid: 3.96 g (82%). ^{1}H NMR (300 MHz, $CDCl_3$, δ in ppm): 1.14 (s, 3H, $-CH_3$), 1.36 (s, 6H, $-CH_3$), 1.88 (s, 3H, $-CH_3$), 3.56 (d, 2H, $-CH_2O$), 4.10 (d, 2H, $-CH_2O$), 4.31 (t, 4H, $-CH_2O$).

2.3.3. Typical copolymerization procedure: PMMA-s-PIMPHMA (**A2**)

EBiB (4.5 μL, 0.033 mmol), IMPHMA (4.29 g, 15 mmol), MMA (0.5 g, 5 mmol), $CuBr_2$ (0.0002 g, 0.001 mmol), PMDETA (3.5 μL, 0.016 mmol), and anisole (2.5 mL) were added to a 25 mL Schlenk flask. The flask was deoxygenated by five freeze–pump–thaw cycles. CuBr (2.3 mg, 0.016 mmol) was added to the frozen mixture in the presence of argon. The flask was filled with argon and heated in an oil bath at 70 °C. Polymerization was stopped 5 h later by exposing the solution to air. The resulting solution was passed through neutral alumina to remove the copper complex. The polymer was precipitated twice in hexane and dried under vacuum at room temperature for 24 h.

2.3.4. Deprotection: PMMA-s-(PIMPHMA-OH) (**B2**)

1.0 g of PMMA-*s*-PIMPHMA was dissolved in 20 mL of THF and methanol mixture (ratio = 7:3). The solution pH was maintained around 3 while 0.1 N HCl was added drop-wise to a flask. The reaction mixture was stirred for 24 h at room temperature. The resulting reaction mixture was precipitated into diethyl ether and dried under high vacuum at room temperature for 24 h.

2.3.5. Functionalization with ATRP initiation groups: PMMA-s-(PIMPHMA-Br) (**C2**)

PMMA-*s*-(PIMPHMA-OH) (0.97 g, 4 mmol of OH groups), bromo-2-methyl propanoic acid (2.01 g, 12 mmol), DCC (2.47 g, 12 mmol), and DMF (8 mL) were placed in a 25 mL round-bottom flask. The flask was sealed and kept in an ice bath. The reaction mixture was stirred for 40 h at room temperature. The resulting reaction mixture was filtered and precipitated into methanol/water (80/20 w/w). The precipitate was redissolved in 10 mL of $CHCl_3$, precipitated into hexane, and dried under vacuum at room temperature for 24 h.

2.3.6. Typical brush polymerization procedure of PMMA-s-[(PIMPHMA-g-PBA)] (**D2**)

PMMA-*s*-(PIMPHMA-Br) (**C2**) (0.11 g, assumed to contain 0.5 mmol of initiating groups), n-BA (28.8 g, 200 mmol), anisole (3.0 mL), $CuBr_2$ (0.0005 g, 0.025 mmol), and dNbpy (0.20 mg, 0.5 mmol) were added to a 50-mL Schlenk flask. The reaction mixture was degassed by three freeze–pump–thaw cycles. After stirring for 0.5 h at room temperature, CuBr (0.038 g, 0.25 mmol) was added under nitrogen, and the flask was placed in a preheated oil bath at 70 °C. Polymerization was stopped after 40 h by cooling the flask to room temperature and opening the flask to air. The resulting polymer solution was purified by passing through a column of neutral alumina. The solvent and remaining monomer were removed under high vacuum (1 mmHg). The resulting product was dried at room temperature for 12 h.

2.3.7. Typical procedure for side chain hydrolysis

PMMA-*s*-[(PIMPHMA-*g*-PBA)] (**D2**) (25 mg) was dissolved in THF (1.5 mL) and 1-butanol (8.5 mL). Concentrated sulfuric acid (4 drops) was added, and the solution was heated at 100 °C for 7 days. The solvent was removed under vacuum, and the remaining residue was dissolved in $CHCl_3$ (5 mL). After extracting with water (2 mL), the organic layer was isolated and vacuum-distilled at room temperature. The resulting polymer was characterized by GPC, which indicated nearly quantitative cleavage.

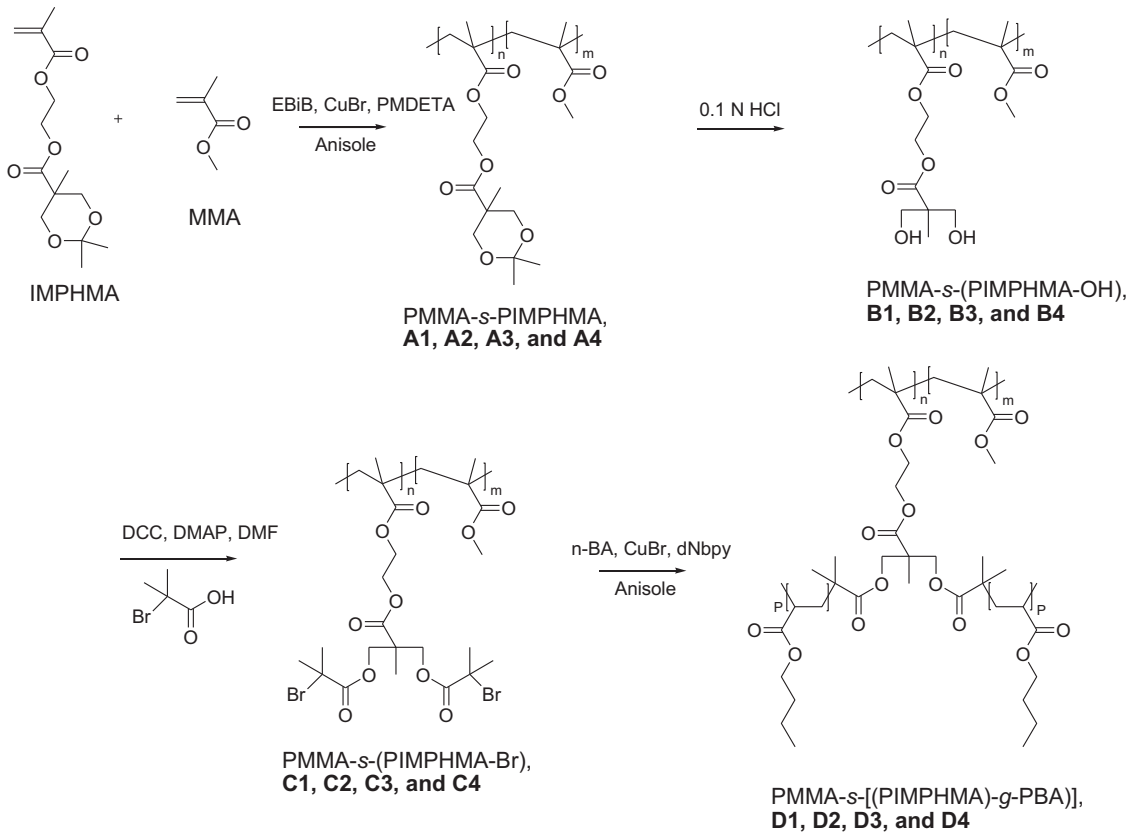

Scheme 1. Synthesis of molecular brushes containing PBA in the side chains from a series of [PMMA-*s*-(PIMPHMA-Br)] backbones.

3. Results and discussion

Scheme 1 outlines the synthetic route for preparing densely grafted brushes with PBA side chains. Esterification was carried out with HEMA and I-Bis-MPA in the presence of EDC and DMAP to yield a novel monomer, IMPHMA, which could be derivatized to have an initiating moiety for brush synthesis. Copolymerization of IMPHMA and MMA with different molar ratios of 50:50, 75:25, 90:10, and 100:0 was carried out to prepare a series of [PMMA-*s*-(PIMPHMA)] copolymers (**A1**, **A2**, **A3**, and **A4**) with different grafting densities along the backbone. Evidence for the controlled nature of IMPHMA and MMA copolymerization was obtained by GPC (Fig. 1 and supporting information). The representative example of copolymerization (IMPHMA:MMA = 75:25) that led to copolymer **A2** is shown in Fig. 1a. An increase in molecular weight with increasing conversion is observed, which is qualitatively indicative of the molecular weight increasing throughout the polymerization. The controlled nature of copolymerization is supported by the fact that polydispersity remained low during the entire polymerization, as shown in Table 1. The resulting copolymers were also analyzed by ^{1}H NMR spectroscopy to observe their copolymer composition in the backbone. The final composition of copolymer **A2** was calculated from the integral intensities of the (a) $-OCH_3$ group peak (3.58 ppm) in MMA and the (b) $-OCH_2$ group peak (4.36 ppm) in IMPHMA (Fig. 2). Results from four copolymerizations are summarized in Table 1.

In the next step, the deprotection reaction was carried out in a mixed solvent of THF and methanol (7:3 ratio). Then 0.1 N HCl was added to the solution until solution pH reached 3. I-bis-MPA groups present in a series of copolymer **A** were deprotected to

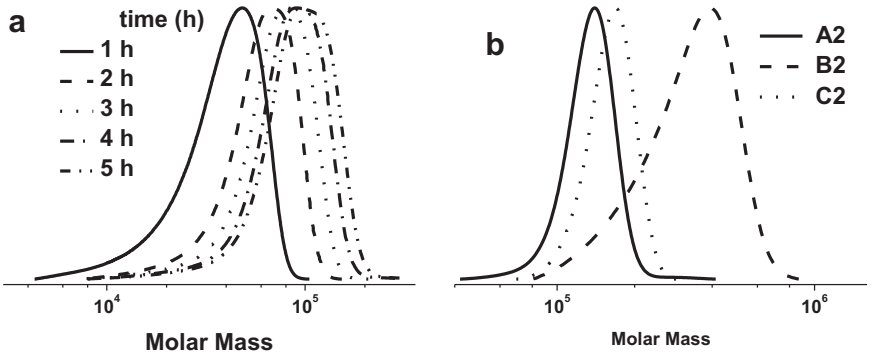

Fig. 1. GPC traces for a) the copolymerization of IMPHMA and MMA (**A2**), b) a backbone PMMA-*s*-PIMPHMA (75% of IMPHMA along the backbone) (**A2**), a deprotected product PMMA-*s*-(PIMPHMA-OH) (**B2**), and a macroinitiator PMMA-*s*-(PIMPHMA-Br) (**C2**).

Table 1
Reaction conditions and results for the copolymerization of MMA and IMPHMA.

Entries	$[M_1]:[M_2]:[I]:[Cu^+]:[Cu^{2+}]:[L]$[a]	Conv[b] (%)		Incorporation ratio $(M_1:M_2)$[c]	DP[b]		$M_{n,\ theo}$ ($\times 10^{-4}$)	$M_{n,\ app}$[d] ($\times 10^{-4}$)	PDI[d]
		M_1	M_2		M_1	M_2			
A1	300:300:1:0.5:0.025:1	62	65	47:53	186	195	7.3	8.4	1.08
A2	450:150:1:0.5:0.025:1	70	75	74:26	315	113	10.1	13.1	1.11
A3	540:60:1:0.5:0.025:1	75	72	88:12	405	43	12.0	14.0	1.12
A4	600:0:1:0.5:0.025:1	48	–	100:0	288		11.2	21.3	1.20

[a] M_1 = IMPHMA, M_2 = MMA, I = EBiB, Cu^+ = CuBr, Cu^{2+} = $CuBr_2$, L = PMDETA.
[b] Obtained from gas chromatography.
[c] Calculated from NMR results.
[d] Determined by GPC in DMF with PMMA calibration.

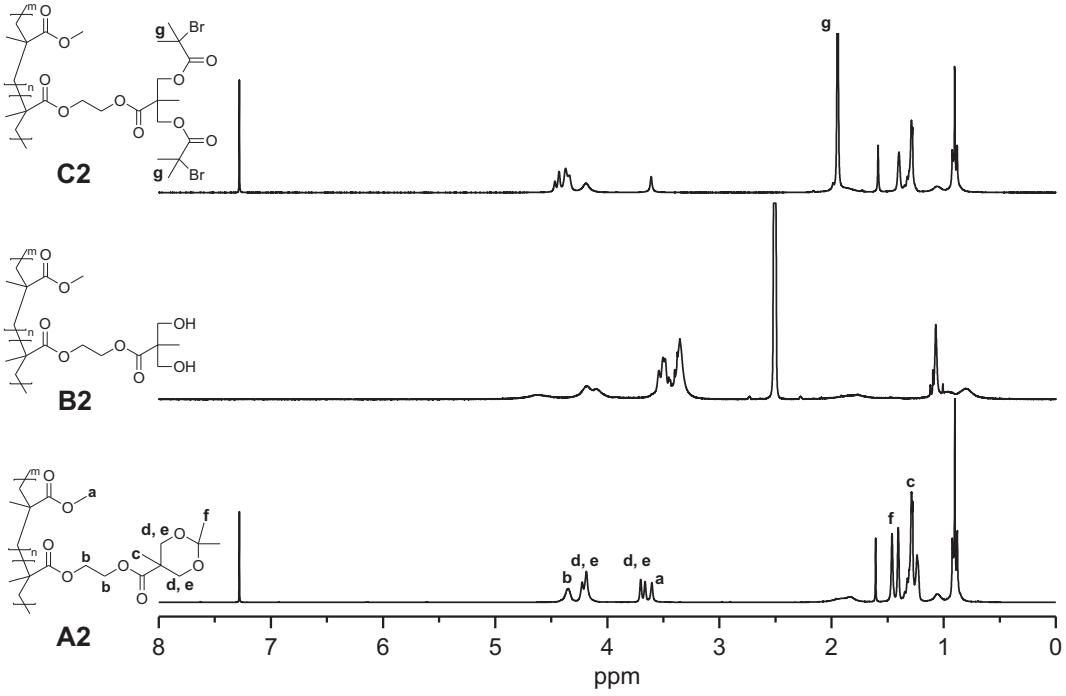

Fig. 2. 1H NMR spectra of a backbone PMMA-*s*-PIMPHMA (75% of IMPHMA along the backbone) (**A2**), a deprotected product PMMA-*s*-(PIMPHMA-OH) (**B2**), and a macroinitiator PMMA-*s*-(PIMPHMA-Br) (**C2**).

form hydroxyl side groups, yielding a series of copolymer **B**. The resulting copolymers were not soluble in THF or chloroform, which indicates successful deprotection. Esterification reactions between the resulting copolymers and 2-bromo-2methyl propionic acid were carried out to introduce an ATRP initiating group at the end of the repeating unit. ^{1}H NMR and GPC were used to analyze the deprotection and functionalization processes. The ^{1}H NMR spectrum provided evidence of the complete transformation of the terminal hydroxyl groups to ATRP initiation groups. As shown in Fig. 2, the disappearance of the peak (f) of a I-Bis-MPA methyl group at 1.36 ppm and the complete change in solubility supported the transformation into hydroxyl groups. After esterification, a series of copolymer **C** became soluble again in THF or chloroform and the peak (g) appeared in the NMR, demonstrating successful loading of the ATRP initiation groups. After deprotection, the apparent molecular weight of **B2** increased about two-fold compared to that of **B2.** This discrepancy could be attributed to the difference in hydrodynamic volumes between two polymers with respect to PMMA in DMF (Fig. 1b) [34]. After esterification, the apparent molecular weight of **C2** became similar to that of **A2**, indicating successful transformation (Fig. 1 and supporting information).

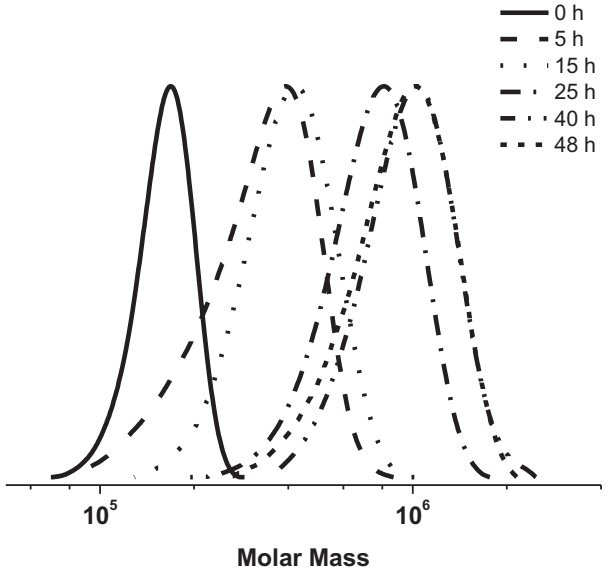

Fig. 3. GPC traces during the syntheses of PMMA-*s*-[(PIMPHMA-*g*-PBA)] brushes (**D2**) (5–48 h) from a macroinitiator PMMA-*s*-(PIMPHMA-Br) (**C2**) (0 h).

Table 2
Results of *n*-Butyl Acrylate (BA) Polymerization from a series of [PMMA-*s*-(PIMPHMA-Br)] backbones.

Brushes	Macroinitiators	Time (h)	Conv (%)[a]	$DP_{n,SC\text{-}theory}$[b]	$M_{n,\ theory}$[c]	$M_{n,\ app}$[d]	PDI[d]
D1	C1	5	1.8	7	333,000	192,000	1.18
		15	2.8	11	524,000	241,000	1.15
		25	5.5	22	1,048,000	385,000	1.19
		40	8.3	33	1,571,000	528,000	1.19
D2	C2	5	1.3	5	403,000	221,000	1.21
		15	2.0	8	645,000	382,000	1.25
		25	5.0	20	1,613,000	723,000	1.24
		40	7.5	30	2,420,000	920,000	1.20
D3	C3	5	1.0	4	415,000	320,000	1.25
		15	2.8	11	1,140,000	611,000	1.28
		25	4.0	16	1,659,000	796,000	1.26
		40	5.8	23	2,385,000	1,130,000	1.26
D4	C4	5	1.3	5	369,000	239,000	1.31
		15	4	16	1,180,000	510,000	1.35
		25	5.3	21	1,548,000	630,000	1.34
		40	8.8	35	2,580,000	1,310,000	1.37

[a] Obtained from gas chromatography.
[b] Calculated from $DP_{n,SC\text{-}theory}$ = ([BA]/[PMMA-*s*-(PIMPHMA-Br)]) × conversion.
[c] Calculated from $M_{n,\ theory}$ = ([BA]/[PMMA-*s*-(PIMPHMA-Br)]) × (molecular weight)$_{BA}$ × conversion.
[d] Determined by GPC in DMF with PMMA calibration.

Table 3
Results of side chains cleaved from PMMA-*s*-[(PIMPHMA-*g*-PBA)] brushes.

Brushes	Time (h)	Conv (%)[a]	$M_{n,SC\text{-}theory}$[b]	$M_{n,SC\text{-}cleaved}$[c]	$DP_{n,SC\text{-}theory}$[d]	$DP_{n,SC\text{-}cleaved}$[e]	PDI[c]	f[f]
D1	5	1.8	900	1730	7	14	1.18	52
	15	2.8	1400	2140	11	17	1.15	69
	25	5.5	2800	3700	22	29	1.19	76
	40	8.3	4200	4580	33	36	1.19	92
D2	5	1.5	640	2000	5	16	1.21	32
	15	2.0	1020	2340	8	18	1.25	44
	25	5.0	2560	3920	20	31	1.24	65
	40	7.5	3840	4520	30	35	1.20	85
D3	5	1.0	510	1960	4	15	1.25	26
	15	2.8	1400	3270	11	26	1.28	43
	25	4.0	2050	3690	16	29	1.26	56
	40	5.8	2950	4900	23	38	1.26	60
D4	5	1.3	640	2790	5	22	1.31	23
	15	4	2048	6440	16	50	1.35	32
	25	5.3	2680	7680	21	60	1.34	35
	40	8.8	4480	8600	35	67	1.37	52

[a] Obtained from gas chromatography.
[b] $M_{n,SC} = M_n$ of the side chain, $M_{n,SC\text{-}theory} = (M_{n,brush} - M_{n,[PMMA\text{-}s\text{-}(PIMPHMA\text{-}Br)]})/DP_{n,[PMMA\text{-}s\text{-}(PIMPHMA\text{-}Br)]}$.
[c] Determined by GPC in DMF with PMMA calibration.
[d] Calculated from $DP_{n,SC\text{-}theory}$ = ([BA]/[PMMA-*s*-(PIMPHMA-Br)]) × conversion.
[e] Calculated from $DP_{n,SC\text{-}cleaved} = M_{n,SC\text{-}cleaved}/(\text{molecular weight})_{BA}$.
[f] Initiation efficiency calculated from $f = M_{n,SC\text{-}theory}/M_{n,SC\text{-}cleaved}$.

A series of molecular brushes (**D1**, **D2**, **D3**, and **D4**) were synthesized by grafting *n*-BA from a series of backbones (**C1**, **C2**, **C3**, and **C4**) (Scheme 1). As shown in Fig. 3, the GPC traces for **D2** synthesis shifted continuously toward higher molecular weight throughout the polymerization due to both the propagation from the main chain and the side chain. No high molecular weight shoulder was observed when compared with that of the macroinitiator (**C2**), indicating no evidence for intermolecular brush–brush coupling. The brush syntheses appeared to proceed in a controlled fashion because the polydispersities for all cases remained low. Results from the brush synthesis are summarized in Table 2.

To investigate the influence of the steric congestion of the initiation sites on the initiation efficiency during molecular brush synthesis, the side chains of a series of molecular brushes (**D1**, **D2**, **D3**, and **D4**) were cleaved by acid hydrolysis in 1-butanol at 100 °C. It has been previously demonstrated that complete side chain cleavage occurs under these conditions while retaining the ester functionalities of each monomer unit. A series of cleaved side chains were then characterized by GPC to examine initiation

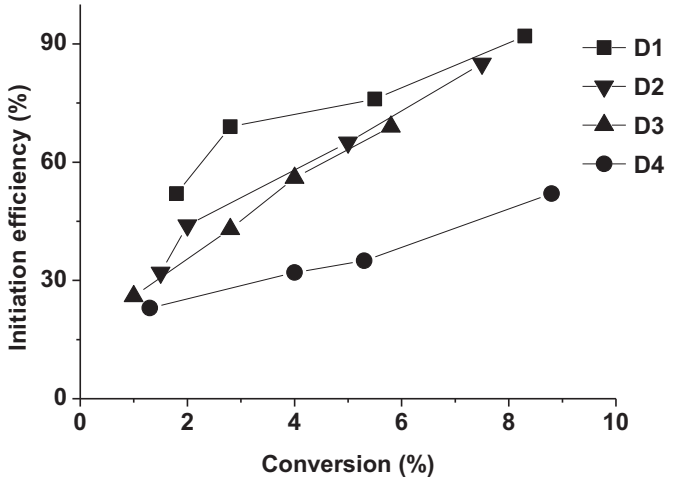

Fig. 4. Initiation efficiency as a function of conversion for a series of brushes (**D1** ~ **D4**).

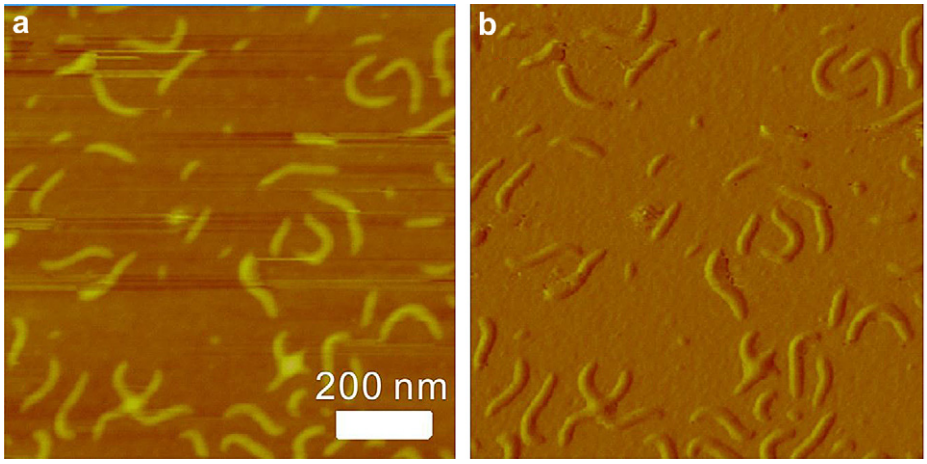

Fig. 5. (a) Height and (b) amplitude-mode AFM images of the D4 brushes adsorbed onto a silicon wafer. The z-scale of the height is 30 nm and phase is 50°, respectively.

efficiency during the growth of side chains. Molecular weights for the cleaved side chains were calculated using a conventional calibration based on linear PMMA standards (Table 3). Initiation efficiency is, in principle, defined as the ratio of the actual initiating sites to the total number of Br initiation groups. The initiation efficiency (f) can be also obtained by the ratio between $M_{n,SC\text{-}theory}$ and $M_{n,SC\text{-}cleaved}$ ($f = M_{n,SC\text{-}theory}/M_{n,SC\text{-}cleaved}$) [26]. For all cases, f is low in the early stage of polymerization (23–52 %). It usually increased with the progress of polymerization and reached 52–92 %. The side chains that begin growing early from a fraction of the initiation sites sterically hinder the initiation sites of adjacent repeating units of the backbone. This causes noncomplete initiation at the initial time. Fig. 4 shows that f gradually increases with monomer conversion. It should be noted that as the steric hindrance of the initiation sites increases, f decreases. For example, f of **D4** with the highest steric hindrance of the initiation sites is initially similar to those of **D2** and **D3**. However, it becomes the least sterically hindered among the four brushes as polymerization progresses. A comparison between the initiation efficiencies of four brushes demonstrated that increases in steric hindrance of the initiation sites during brush synthesis prevented the side chains from growing efficiently and decreased the overall initiation efficiency.

Atomic force microscopy (AFM) offers a facile access to the structural information of polymer brushes prepared through direct visualization of molecular structures [35,36]. As a representative brush, we have measured the D4 brushes of [PMMA-*s*-(PIMPHMA-*g*-PBA)] with a highest degree of branches. As shown in Fig. 5, the diluted solution of D4 brush deposited on a silicon wafer exhibits a wormlike morphology similar to that of previous report. Unlike the crystalline brushes, the amorphous brushes of PBA chain serve to the adsorption of the side chains on the surface without altering the molecular conformation, resulting in the clear separation of individual macromolecular brushes. In addition, we found that the average diameter and contour length of the D4 brush correspond to 35 ± 2.5 nm and 166 ± 17 nm (averaged over 50 samples), which are in good agreement with the theoretical calculations based on the molecular weights and degree of branches measured in GPC.

4. Conclusions

Well-defined macroinitiators with different initiation site densities were synthesized by the copolymerization of IMPHMA and MMA followed by deprotection and transformation into PMMA-PIMPHMA-Br. These macroinitiators exhibited a statistical spacing of ATRP initiating groups along the backbone ranging from 50 to 100 %. From these macroinitiators, molecular brushes with densely grafted PBA side chains were synthesized using the grafting-from strategy by ATRP. The synthesized molecular brushes were of high molecular weight and relatively low polydispersities. The initiation efficiencies of the ATRP processes were determined by cleaving the side chains and performing GPC analysis. In the early stage of polymerization, the initiating efficiencies of four brushes ranged from 23 to 52 % but reached around 52–92 % in the final stage of polymerization. Initiation efficiency decreased with increasing density of initiation groups along the backbone. This result demonstrated that slow initiation was caused by steric hindrance. AFM demonstrated that the molecular brushes adsorbed on the mica surface have a wormlike structure. Ongoing experiments will focus on the rate of adsorption-induced degradation of molecular brushes as a function of grafting density, offered by the different density of the side chains.

Acknowledgments

This work was supported by the WCU research program (R31-2008-000-20012-0), Priority Research Center Program (2009-0093818), and Basic Science Research Program (2010-0008642) through the National Research Foundation of Korea funded by the Ministry of Education, Science, and Technology of Korea.

Appendix A. Supporting information

Supplementary data associated with this article can be found, in the online version, at http://dx.doi.org/10.1016/j.polymer.2012.06.008.

References

[1] Matyjaszewski K. Prog Polym Sci 2005;30(8–9):858–75.
[2] Lee H-i, Pietrasik J, Sheiko SS, Matyjaszewski K. Prog Polym Sci 2010;35(1–2):24–44.
[3] Sheiko SS, Sumerlin BS, Matyjaszewski K. Prog Polym Sci 2008;33(7):759–85.
[4] Zhang M, Mueller AHE. J Polym Sci Part A Polym Chem 2005;43(16):3461–81.
[5] Dziezok P, Sheiko SS, Fischer K, Schmidt M, Moller M. Angew Chem Int Ed 1997;36(24):2812–5.
[6] Pakula T, Zhang Y, Matyjaszewski K, Lee H-i, Boerner H, Qin S, et al. Polymer 2006;47(20):7198–206.
[7] Zhang M, Estournes C, Bietsch W, Mueller AHE. Adv Funct Mat 2004;14(9):871–82.
[8] Huang J, Tang C, Lee H, Kowalewski T, Matyjaszewski K. Macromol Chem Phys 2007;208(21):2312–20.

[9] Tang C, Dufour B, Kowalewski T, Matyjaszewski K. Macromolecules 2007; 40(17):6199–205.
[10] Rzayev J. Macromolecules 2009;42(6):2135–41.
[11] Xia Y, Olsen BD, Kornfield JA, Grubbs RH. J Am Chem Soc 2009;131(51): 18525–32.
[12] Park I, Sheiko SS, Nese A, Matyjaszewski K. Macromolecules 2009;42(6): 1805–7.
[13] Sumerlin BS, Matyjaszewski K. Macromol Eng 2007;2:1103–35.
[14] Rathgeber S, Pakula T, Wilk A, Matyjaszewski K, Beers KL. J Chem Phys 2005; 122(12). 124904/124901-124904/124913.
[15] Rathgeber S, Lee H-I, Matyjaszewski K, Di Cola E. Macromolecules 2007; 40(21):7680–8.
[16] Sheiko SS, Sun FC, Randall A, Shirvanyants D, Rubinstein M, Lee H-i, et al. Nature 2006;440(7081):191–4.
[17] Park I, Nese A, Pietrasik J, Matyjaszewski K, Sheiko SS. J Mater Chem 2011; 21(23):8448–53.
[18] Lebedeva NV, Sun FC, Lee H-i, Matyjaszewski K, Sheiko SS. J Am Chem Soc 2008;130(13):4228–9.
[19] Gao H, Matyjaszewski K. J Am Chem Soc 2007;129(20):6633–9.
[20] Vogt AP, Sumerlin BS. Macromolecules 2006;39(16):5286–92.
[21] Neugebauer D, Zhang Y, Pakula T, Sheiko SS, Matyjaszewski K. Macromolecules 2003;36(18):6746–55.
[22] Ishizu K, Tsubaki S, Uchida SJ. Macromol Sci. Pure Appl Chem 1995;A32(7): 1227–34.
[23] Beers KL, Gaynor SG, Matyjaszewski K, Sheiko SS, Moeller M. Macromolecules 1998;31(26):9413–5.
[24] Lee H, Jakubowski W, Matyjaszewski K, Yu S, Sheiko SS. Macromolecules 2006;39(15):4983–9.
[25] Lee H-i, Matyjaszewski K, Yu-Su S, Sheiko SS. Macromolecules 2008;41(16): 6073–80.
[26] Sumerlin BS, Neugebauer D, Matyjaszewski K. Macromolecules 2005;38(3): 702–8.
[27] Matyjaszewski K, Xia J. Chem Rev 2001;101(9):2921–90.
[28] Wang J-S, Matyjaszewski K. J Am Chem Soc 1995;117(20):5614–5.
[29] Braunecker WA, Matyjaszewski K. Prog Polym Sci 2007;32(1):93–146.
[30] di Lena F, Matyjaszewski K. Prog Polym Sci 2010;35(8):959–1021.
[31] Kamigaito M, Ando T, Sawamoto M. Chem Rev 2001;101(12):3689–746.
[32] Tsarevsky Nicolay V, Matyjaszewski K. Chem Rev 2007;107(6):2270–99.
[33] Malkoch M, Malmstroem E, Hult A. Macromolecules 2002;35(22):8307–14.
[34] Jung S-H, Song H-Y, Lee Y, Jeong HM, Lee H-i. Macromolecules 2011;44(6): 1628–34.
[35] Sheiko SS, da Silva M, Shirvaniants D, LaRue I, Prokhorova S, Moeller M, et al. J Am Chem Soc 2003;125(22):6725–8.
[36] Sheiko SS, Moeller M. Chem Rev 2001;101(12):4099–123.